

Comparison of divertor power loads of spontaneous and pellet triggered ELMs at JET

R. Wenninger¹, T. Eich¹, W. Fundamenski², P. T. Lang¹, S. Devaux¹, K. Gál³, A. Geraud⁴, D. Harting⁵, G. Kocsis³, H.W. Müller¹, H. Thomsen¹ and JET-EFDA contributors*

JET-EFDA, Culham Science Centre, OX14 3DB, Abingdon, OXON, United Kingdom

¹ *Max-Planck-Institut für Plasmaphysik, EURATOM Association, Boltzmannstr. 2, 85748 Garching, Germany*

² *EURATOM-UKAEA Fusion Association, Culham Science Centre, Abingdon, UK*

³ *MTA-KFKI-RMKI, EURATOM Association, P.O. Box 49, H-1525 Budapest-114, Hungary*

⁴ *CEA, IRFM, F-13108 Saint-Paul-lez-Durance, France*

⁵ *Institute for Energy Research - Plasma Physics, Forschungszentrum Juelich, Association EURATOM-FZJ, Trilateral Euregio Cluster, 52425 Juelich, Germany*

* *See the Appendix of F. Romanelli et al., Fusion Energy 2008 (Proc. 22nd IAEA Conf., Geneva, 2008)*

1. Introduction

It is currently assumed that a reliable technique for the mitigation of Edge Located Modes (ELMs) is mandatory for the success of ITER. The severity of the ELM impact on the divertor plasma-facing components is determined by ELM rise time, wetted area and energy deposited on the divertor targets during the ELM rise time. For any candidate control technique to mitigate ELMs to 1MJ detailed analysis of divertor power load characteristics has to be carried out. Experiments at ASDEX Upgrade have shown that by Pellet ELM pacing [1] ELMs can be triggered reliably up to frequencies twice the natural ELM frequency. We present a comparison of several divertor power load aspects of spontaneous and pellet triggered ELMs employing infrared thermography [2].

2. Experimental Setup

Currently a new pellet injection system for JET is in the phase of commissioning. The High Frequency Pellet Injector (HFPI) was designed to deliver small ($0.7 - 1.3 \times 10^{20}$ D) pellets at a rate of up to 60 Hz and in the speed range 50 – 200 m/s for Pellet ELM Pacing and large ($24 - 40 \times 10^{20}$ D) pellets up to 15 Hz and 100 – 500 m/s for Deuterium Fuelling [3]. For the experiments described here large pellets with a nominal particle content of 2.4×10^{21} D have been used. Pellets produced by the HFPI were guided in our experiments via the flight line, which is associated with a normal injection from the magnetic low field side (LFS). Due to the High- β Plasmoid Drift [4], which for LFS injection leads to a low fuelling efficiency compared to injection from the high field side, this injection direction is regarded as favourable for pellet ELM pacing with minimal fuelling. The LFS injection line is equipped with a microwave cavity for pellet detection 3.4m before the vessel.

A new divertor infrared camera has been extensively exploited in these studies. It has a slim rectangular view on the divertor elongated in the poloidal direction and a temporal resolution from $\sim 30\mu\text{s}$ (reduced poloidal extension) to $\sim 90\mu\text{s}$ (full view). Its spatial resolution is 1.63mm respectively 5.0mm for the observable area on the outer respectively inner divertor.

3. Comparison of general ELM power load aspects

For the analysis described below a high triangularity H-mode discharge (JPN 76697) with $I_p=2.5\text{MA}$, $B_t=2.7\text{T}$, $q_{95}=3.4$, $P_{\text{NBI}}\approx 13\text{MW} / 16.5\text{MW}$ has been performed. The discharge is optimised for divertor power load analysis employing the divertor IR camera with a time resolution of $86\mu\text{s}$. Therefore, the strike points were positioned in a way that the full outer power deposition but less than one decay length on the inner divertor have been observed. Fig. 1 shows time traces describing main discharge parameter between 18s and 22s. Before the start of pellet injection type I ELMs with an average frequency of ~ 10 Hz are observed. From 17.5s to 22s pellets are fired at 10Hz frequency and a velocity of about 150m/s.

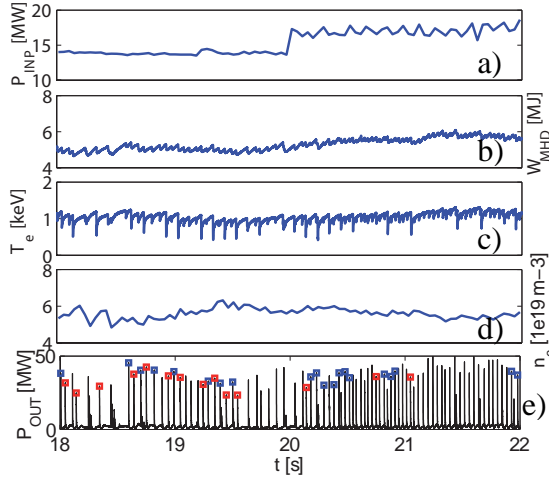


Fig. 1: JPN 76697 (18-22s) – main discharge parameter: a) input power, b) thermal energy, c) and d) pedestal values of T_e and n_e e) power to outer divertor - squares: analysed spontaneous (blue) and triggered (red) ELMs

density on the outer strike plate evaluated by IR calculates for all selected ELMs the three times $t_{\text{ELM,start}}$, $t_{\text{ELM,max}}$ and $t_{\text{ELM,end}}$. In Fig. 3 average values of these times are indicated. The selected sets of ELMs have similar average time intervals to the ELM before (spont. 44ms, trig. 39ms) and similar average plasma energies at $t_{\text{ELM,start}}$ (spont. 5.4MJ, trig. 5.2MJ).

3.1. Thermal energy losses and radiated energy

For the evaluation of the ELM associated loss of thermal energy for both diamagnetic energy (ΔW_{DIA}) and thermal energy acquired via the equilibrium code EFIT (ΔW_{MHD}) the mean values at $t_{\text{ELM,end}}$ are subtracted from the mean values at $t_{\text{ELM,start}}$. This approach tends to underestimate the loss of thermal energy due input power constantly raising the thermal energy. However for both spontaneous and triggered ELMs comparable amounts of input energy (W_{INP}) have entered the plasma between $t_{\text{ELM,start}}$ and $t_{\text{ELM,end}}$ ($78 \pm 10 \text{ kJ}$ resp. $72 \pm 6 \text{ kJ}$). Spontaneous ELMs ($\Delta W_{\text{DIA}} = 151 \pm 46 \text{ kJ}$, $\Delta W_{\text{MHD}} = 154 \pm 50 \text{ kJ}$) show significantly lower loss of thermal energy compared to losses during pellet triggered ELMs ($\Delta W_{\text{DIA}} = 259 \pm 40 \text{ kJ}$, $\Delta W_{\text{MHD}} = 249 \pm 42 \text{ kJ}$).

The amount of energy radiated between $t_{\text{ELM,start}}$ and $t_{\text{ELM,end}}$ (ΔW_{RAD}) has been integrated from bolometry data (temporal resolution: 0.2ms). Again clearly lower values have been found for spontaneous ELMs ($\Delta W_{\text{RAD}} = 113 \pm 20 \text{ kJ}$) than for triggered ELMs ($\Delta W_{\text{RAD}} = 218 \pm 33 \text{ kJ}$). However especially for the ELM rise phase it can not be assumed that the higher amount of released thermal energy for pellet triggered ELMs is balanced by radiation [5].

From the edge channel of the interferometer the pellet associated fast density increment has been acquired, which is assumed to be roughly proportional to the pellet mass. As Fig. 2a

14 pellet triggered and 21 spontaneous type I ELMs, which are interleaved in the period between 18s and 22s (Fig. 1e), have been identified on the basis of the following ELM selection criteria. Generally only ELMs appearing more than 30ms after their predecessor have been considered to ensure a minimum in comparability of pedestal conditions. ELMs are classified as pellet triggered, if the flight time between pellet detection by microwave cavity in the flight tube and ELM detection in the plasma correspond to the measured pellet velocity plus if, a significant density jump is observed on the edge channel of the interferometer. ELMs, for which just one of these criteria is met, have been excluded from the comparison. All other ELMs have been classified as spontaneous. A standard algorithm using power and the maximum power flux

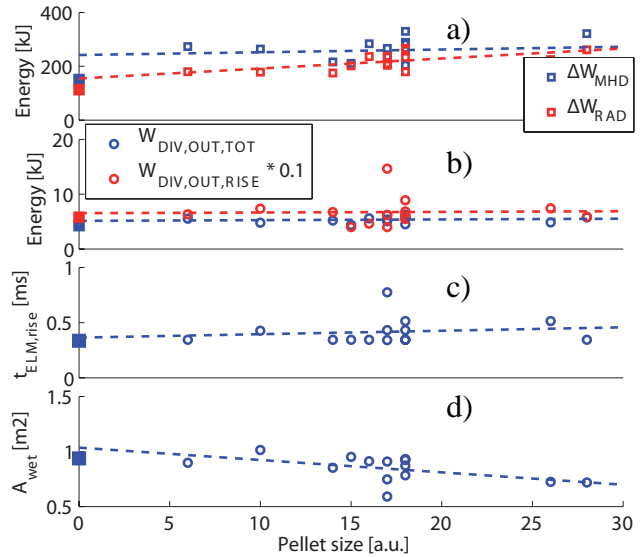


Fig. 2: Scaling with pellet size (edge density increment): a) ΔW_{MHD} and ΔW_{RAD} b) $W_{\text{DIV,OUT,RISE}}$ and $W_{\text{DIV,OUT,TOT}}$ c) $t_{\text{ELM,max}} - t_{\text{ELM,start}}$ d) average wetted area for entire ELM phase. Dashed lines indicate linear regressions, squares represent respective mean values of spontaneous ELMs

shows, for a variation of the density jump by a factor of 5 only a weak scaling of ΔW_{MHD} and ΔW_{RAD} has been found. For ΔW_{MHD} the extrapolation of the linear fit to zero density increment is clearly above the values for spontaneous ELMs.

3.2. Deposition on the outer divertor target

The deteriorating effect of ELMs on the divertor targets roughly can be expressed via the temperature increase ΔT_{ELM} due to a single ELM, which in approximation is a function of thermal material properties $C_{\text{thermal,mater}}$, timescales of the ELM rise phase $\tau_{\text{ELM,RISE}}$, wetted area A_{ELM} and the energy $E_{\text{TAR,RISE}}$ deposited on the target during the ELM rise phase [6]:

$$\Delta T_{\text{ELM}} \approx C_{\text{thermal,mater}} \times E_{\text{TAR,RISE}} / (A_{\text{ELM}} \times \text{sqrt}(\tau_{\text{ELM,RISE}}))$$

Making use of the high spatial resolution of the IR system at the outer target the non material related quantities for this area have been analysed in further detail.

Fig. 3 shows a comparison of the power deposition dynamics on the outer target of the investigated ELMs. Time traces for each ELM have been aligned by $t_{\text{ELM,max}}$. Subsequently averages over both sorts of ELMs have been taken. The ELM rise time ($t_{\text{ELM,max}} - t_{\text{ELM,start}}$) for pellet triggered ELMs ($0.47 \pm 0.18 \text{ms}$) is higher by about 30% in relation to spontaneous ELMs ($0.36 \pm 0.11 \text{ms}$). At the same time triggered ELMs show a slower decay, which is temporarily almost linear and not exponential in time as for the spontaneous ELMs. Fig. 2c shows that both ELM rise time and duration of the full ELM do not scale significantly with the pellet size.

Assuming toroidal homogeneity the wetted area A_{ELM} can be calculated as the relation between the power and the maximum power flux density of the deposition on the divertor target. Accounting for the ELM rise phase ($t_{\text{ELM,max}} - 0.34 \text{ms}$ to $t_{\text{ELM,max}}$) resp. a longer phase including the early part of the decay phase ($t_{\text{ELM,max}} - 0.34 \text{ms}$ to $t_{\text{ELM,max}} + 0.69 \text{ms}$) yields for spontaneous ELMs a wetted area on the outer divertor target of 0.50m^2 resp. 0.76m^2 and for pellet triggered ELMs 0.60m^2 resp. 0.65m^2 . Thus during the crucial ELM rise phase the investigated pellet triggered ELMs have a slightly lower wetted area. This difference in A_{ELM} is stronger for the early rise phase and vanishes towards $t_{\text{ELM,max}}$. Power flux deposition profiles averaged over the described phases are illustrated in Fig. 4.

For the investigated pellet triggered ELMs the maximum power deposited on the outer target is lower (spont.: $29 \pm 4 \text{MW}$, trig.: $26 \pm 5 \text{MW}$) than for their spontaneous counterparts, although the earlier ones are associated with an about 60% higher release of thermal energy.

Nevertheless due to their slower dynamics pellet triggered ELMs are associated with the higher power deposition in the earlier part of the ELM rise phase (and in the later part of the decay phase). Due to this pellet triggered ELMs are associated with a higher energy $W_{\text{DIV,OUT,RISE}}$ deposited during the rise phase ($t_{\text{ELM,start}}$ to $t_{\text{ELM,max}}$) ($6.9 \pm 2.9 \text{kJ}$) compared to spontaneous ELMs ($5.8 \pm 1.4 \text{kJ}$). As well for the energy deposited during the entire ELM

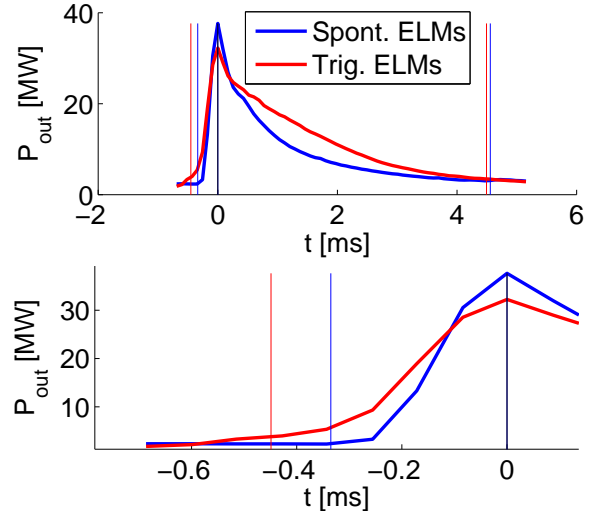


Fig. 3: Comparison of power deposition dynamics (Coherent ELM averaging): a) Complete ELM b) ELM rise phase. Vertical lines indicate averages of $t_{\text{ELM,start}}$, $t_{\text{ELM,max}}$ and $t_{\text{ELM,end}}$ for both sorts of ELMs

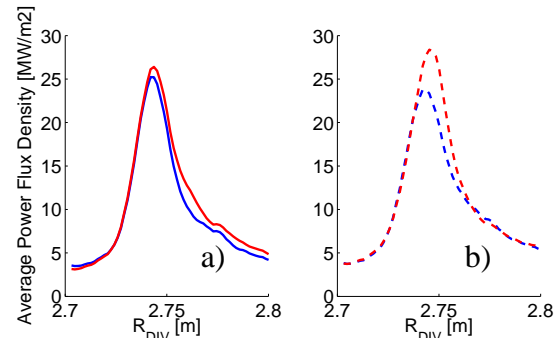


Fig. 4: Average power flux densities for spontaneous (blue) and pellet triggered ELMs (red): a) $t_{\text{ELM,max}} - 0.34 \text{ms}$ to $t_{\text{ELM,max}}$ b) $t_{\text{ELM,max}} - 0.34 \text{ms}$ to $t_{\text{ELM,max}} + 0.69 \text{ms}$

phase $W_{\text{DIV,OUT,TOT}}$ triggered ELMs ($60 \pm 7 \text{kJ}$) exhibit higher values compared to spontaneous ones ($47 \pm 7 \text{kJ}$). Fig. 2b shows that $W_{\text{DIV,OUT,RISE}}$ and $W_{\text{DIV,OUT,TOT}}$ are not scaling with the pellet size.

3.3. Estimation of energy deposited on the inner divertor target

For JET H-mode plasmas with normal field direction it has been reported [7], that the deposited energy per type-I ELM on the inner target is higher than that on the outer target. Due to the position of the inner strike point in the analysed discharge the energy deposited in this area between $t_{\text{ELM,start}}$ and $t_{\text{ELM,end}}$ (W_{IN}) can only be estimated. For this it has been assumed that W_{IN} equals the energy deposited in the area observed by IR ($W_{\text{IN,IR}}$) multiplied by a constant factor c accounting for the very partial view of the deposition area. The ratio between W_{OUT} and $W_{\text{IN,IR}}$ describing the in-out-balance of the ELM energy deposition up to the factor c is 2.4 ± 0.4 for spontaneous ELMs and 3.6 ± 0.5 for triggered ELMs. This indicates that the latter ones have a similar or a more balanced in-out-symmetry compared to spontaneous ELMs.

4. Nonaxisymmetric Energy Deposition Patterns

The spatial and temporal resolution of the IR measurements especially on the outer target allows observation of deposition peaks, which can be linked to toroidal asymmetric structures in the SOL [8]. As observed before for spontaneous ELMs, for a number of pellet triggered ELMs several statistically distributed and laterally displaced stripes, many of which are well separated from each other and from the main strike zone, have been observed especially during the ELM rise phase. These structures can be interpreted as footprints of helical perturbations at the low field side of the plasma edge, which are approximately aligned with the magnetic field structure. Fig. 5 shows the evolution of the deposition pattern during the rise phase of a pellet triggered ELM from a high triangularity type-I ELMy H-mode discharge.

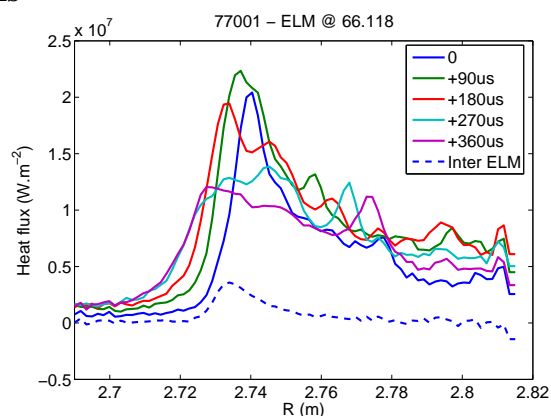


Fig. 5: Development of deposition pattern for a pellet triggered ELM: The times are relative to $t_{\text{ELM,sta}}$

5. Summary

The investigated pellet triggered ELMs in comparison to the spontaneous ELMs show the following features: They are associated with 60% higher losses of thermal energy (not clearly scaling with the pellet size), as well as a higher radiated energy. The energy deposited on the outer target during the ELM rise phase is higher by $\sim 20\%$, while the wetted area during this phase is slightly lower. The ELM rise time is higher by $\sim 30\%$.

There is an indication that pellet triggered ELMs have a similar or more balanced divertor in-out-symmetry compared to spontaneous ELMs. As for spontaneous ELMs deposition structures have been observed for pellet triggered ELMs, which suggest a toroidally asymmetric component of the SOL transport.

References

- [1] P. T. Lang et al., Nucl. Fusion 43 No 10 (2003) 1110-1120.
- [2] T. Eich et al., P. P. C. F. 49 (2007) 573-604
- [3] A. Geraud et al., Fus. Eng. and Des. 82 (2007) 2183-2188.
- [4] H. W. Müller et al., Phys. Rev. Lett. 83, 2199 (1999).
- [5] P. Monier-Garbet et al., Nucl. Fusion 45 (2005) 1404-1410.
- [6] T. Eich et al., J. Nucl. Mater. 337-339 (2006) 669.
- [7] T. Eich et al., J. Nucl. Mater. 363-365 (2007) 989.
- [8] T. Eich et al., Phys. Rev. Lett. 91, 195003 (2003).

Acknowledgement:

This work, supported by the European Communities under the contract of Association between EURATOM/IPP, was carried out within the framework of the European Fusion Development Agreement. The views and opinions expressed herein do not necessarily reflect those of the European Commission